RSC Advances

ROYAL SOCIETY OF CHEMISTRY

www.rsc.org/advances

RSC Advances

RSCPublishing

PAPER

Programming and use of Parylene-C fluorescence as a quantitative on-chip reference

Cite this: DOI: 10.1039/x0xx00000x

Diego G. Dupouy*, Ata Tuna Ciftlik, Joan Teixidor, and Martin A. M. Gijs

Received 00th January 2012,
Accepted 00th January 2012

DOI: 10.1039/x0xx00000x

www.rsc.org/

A large number of lab-on-a-chip applications use fluorescence for quantifying biological entities. In such applications, incorporation of a stable on-chip fluorescent reference source would be highly desirable in order to compensate for instrumental parameter variations, like for example non-constant illumination intensity over time. In this study, we exploit Parylene-C that is used as bonding layer material in a microfluidic chip. We first show programming of intermediate Parylene-C bonding layer fluorescence (iPBLF) and its characterization as a function of the ultraviolet (UV) dose and Parylene-C thickness. This technique requires no additional steps in the fabrication of the microfluidic chip and the fluorescence reference zones can simply be incorporated by local exposure to UV light after fabrication. Next, we demonstrate a fluorescence-based analyte concentration and flow-rate measurement in a microfluidic channel, under changing experimental conditions of illumination intensity and taking different microscope objectives. Sensing is realized by analyzing programmed reference and channel images by straightforward data handling using an open-source image processing tool. We anticipate that the demonstrated method will be a key technique allowing low complexity and reliable quantitative fluorescent measurements, for example in point-of-care and mobile diagnostic applications, where intensity calibration can present a major challenge.

Introduction

Fluorescence microscopy is widely used as a signal readout method in microfluidic platforms.[1] In many applications, the intensity of the fluorescence signal is used to quantify the extent or concentrations of the biological entities on-chip. One popular application is that of on-chip immunoassays[2], where the obtained fluorescent intensity is used to quantify the target antigen concentration. In addition, the fluorescent intensity obtained from solutions of fluorescently labelled molecules within microchannels can be used to estimate their surface concentration[3]. Other applications include protein expression quantification using Green Fluorescent Protein (GFP)-tagged molecules or immunocytochemical signals.[4] Despite its widespread use, achieving a reliable quantification of the fluorescent signal is not straightforward in practice. The measured fluorescent signal intensity depends on a large number of parameters that are difficult to standardize universally. These parameters can be listed as: (1) variations in the intensity of the light source over time, (2) magnification, numerical aperture, depth-of-focus and transmission spectra of the objectives, (3) absorption in the light path of the microscope, (4) efficiency and transmission spectrum of the fluorescent filters, and (5) pixel size, binning, spectral sensitivity, dark noise and frame rate of the imaging sensor. In order to be independent of these variations, several calibration steps and a meticulous treatment of the data are required, even when using the same microscope hardware.[5–9] A typical approach to build such reference involves the use of fluorescent dyes embedded in a polymer layer,[10–14] a standard technique that implicates difficult preparation steps. Alternatively, a method concerning gelatine-based probes used as phantoms was proposed,[15] but this approach is too specific for the intended purpose of being a generally usable method. Commercially available solutions are also proposed, for example, kits of fluorescent compounds that can be added to the sample. Fluorescent microspheres custom-mounted on glass slides are also proposed as a commercial solution. Although very reliable, most of these techniques require a trained person, long preparation steps to add external compounds, or the exchange of the sample under the microscope. Such kind of calibration is particularly problematic when it comes to microfluidic systems that claim robust mobile or point-of-care applications, and for which the user has less possibilities to calibrate the instrument.

Therefore, if incorporation of a fluorescent on-chip reference next to the measurement point could be realized, this would be an ideal solution for fluorescent lab-on-a-chip applications. Firstly, this would not only prevent removing the sample to acquire the reference image but also would enable numerous analyses where the comparison to the reference is required in real time. Next, read-out of such reference could also immediately correct for temporal variations, like blinking in the intensity of the light, and hence can render each data point comparable, both during the course of a single experiment and when studying multiple samples. Finally, such mobile

diagnostic applications could be run on any image reader without relying on the user for the calibration.

A number of methods that integrate an on-chip fluorescent reference by making use of external materials and additional fabrication steps have been presented in the literature. For example, in one study, Hoi *et al.* incorporated colloidal crystals inside a microchannel system and used them as a reference wavelength calibration line for online optical analysis.[16] However, this approach increases the cost and complexity of devices, by introducing non-standard materials and additional steps in the fabrication protocol. Moreover, placement of the reference to a pre-defined position on the chip constitutes another challenge. Previously, we have demonstrated Si-Pyrex wafer bonding using Parylene-C as an intermediate bonding layer to create high pressure-resistant microfluidic channels[17,18]. In a recent study, we used the fluorescence of the intermediate Parylene-C bonding layer to locally store binary data on-chip by illuminating with UV or green light[19]. We also demonstrated that the autofluorescence signal from the Parylene-C layer could be employed to recover a bleached fluorescent signal[20]. The major advantage of this method relies on the possibility to modify the fluorescence of an existing structural layer just by illuminating with UV light after fabrication, with no additional materials or steps. In addition, a standard mask aligner is sufficient to assure printing of fluorescent references on all devices of a wafer. While this method is also highly promising for incorporation of a quantitative fluorescence reference on-chip, the demonstrated programming technique only showed how to program the fluorescence to define a high and low intensity level, as required by digital information storage. Printing of a quantitative fluorescent reference, on the other hand, requires more precise programming of iPBLF at different wavelengths, and, for reproducibility of the process, the absolute illumination dose required to achieve a specific fluorescence, as well as the Parylene-C thickness should be exactly controlled.
In this paper, we first study in detail the iPBLF programming process using UV illumination, for different Parylene-C layer thicknesses and at multiple positions on a chip. Then, we print on-chip references nearby a microfluidic channel containing fluorescent molecules, and demonstrate that, using the reference, we can correct for externally induced fluctuations of the fluorescent signal, as originating from variations in the intensity of the lamp, or the magnification and numerical aperture of the objective. Moreover, we show that this technique can also be used to determine the flow rate in a microfluidic channel, in which a fluorescent dye is transported.

Material and methods

Microfluidic chip fabrication and integration

The details of Parylene-C bonding technology can be found elsewhere[17,18]. Briefly, a Si substrate with a 2 µm of SiO_2 layer is bonded to a Pyrex wafer using Parylene-C as an intermediate bonding layer. For the present study, a 2, 5 or 10 µm thick Parylene-C layer was coated on the Si substrate and then patterned via an amorphous Si hard mask using O_2 plasma. A second lithographic step was then used to pattern the microfluidic channels, having a cross section of 50 µm x 60 µm, in the Si substrate using Deep Reactive Ion Etching (DRIE). After the removal of the hard mask, the Si wafer was bonded to a cleaned Pyrex wafer. The bonding is performed under vacuum conditions at 280 °C. The inlet and outlet of the channel were etched from the backside of the wafer, and the chips were finally diced.
Figure 1A shows the layout of the microfluidic chip we have used in our experiments: it contains a microfluidic channel with a width of 50 µm, a height of 60 µm and connected to an inlet and an outlet. The white areas represent the parts of the chip, which have been etched and are without Parylene-C coverage, i. e. the microfluidic channel and circular structures, which are used to homogenize the pressure distribution during bonding. Figure 1B is a schematic cross-section of the chip along the A-A' and B-B' profiles of Figure 1A, also showing that the inlet and outlet are etched from the backside of the wafer. A polymethyl methacrylate (PMMA) holder was used as interface with the microfluidic chip via o-rings. Commercial fluidic connectors (IDEX Health & Science, WA, USA) were used to connect the system to a neMESYS low-pressure syringe pump (Cetoni GmbH, Germany) for flowing the liquids through the microfluidic channel.

Fluorescence reference printing and imaging

An automatized upright fluorescent microscope (Axio Imager M2m, Zeiss GmbH, Germany) in combination with a coverslip thickness-corrected 20x (LD Plan-Neofluoar Ph2 Korr, Zeiss GmbH, Germany) or a 10x objective (EC Epiplan-Neofluar, Zeiss GmbH, Germany) was used to illuminate the samples through the 550 µm thick Pyrex in order to program fluorescent patterns. Images were taken using a monochromatic charge coupled device (CCD) camera (AxioCam MRm, Zeiss GmbH, Germany). The light was produced by a 120 W mercury vapour short arc lamp (X-Cite 120 PC Q Microscope Illumination System, Lumen Dynamics, Canada) and the optical spectrum was selected using two different filter sets, as shown in Table 1, according to the dye-specific excitation/emission wavelength combinations. To adjust the light intensity, neutral density (ND) and fluorescence attenuator (FL) filters, included in the microscope, were employed. The UV irradiance power received by the sample was measured with a power meter (Model 306, Optical Associates Inc., CA, USA) calibrated for a wavelength of 365 nm at the beginning of each experiment. The microscope was controlled by AxioVision 40x64 V 4.9.1.0 software (Zeiss GmbH, Germany). The fluorescent images obtained from the experiments were analysed using the open source software ImageJ. As fluorescent molecules in solution, we used fluorescein-isothiocyanate(FITC)-labelled anti-mouse immuno-globulins (IgGs) produced in rabbits (F9137, Sigma Aldrich, USA). The antibodies (12.3 mg/mL) were diluted in a solution of 0.05% V/V Tween in phosphate buffered saline (PBST) and were delivered in the microfluidic channel using the syringe pump.

Table 1 Excitation and emission wavelengths of the filter sets used for the fluorescence experiments and corresponding commercial dyes

Filter set (ex/em color)	Excitation (nm)	Emission (nm)	Corresponding dyes
UV/blue	BP 310-390	LP 420	DAPI, BFP, AF 350
blue/green	BP 450-490	BP 515-565	FITC, AF 488, GFP

BP: band-pass, LP: low-pass, DAPI: diamidino-phenylindole, BFP: blue fluorescent protein, GFP: green fluorescent protein, FITC: fluorescein-isothiocyanate, AF: AlexaFluor®(Molecular Probes, Invitrogen)

Results

On-chip fluorescent reference printing

Initially, we printed a fluorescent pattern, which we call an on-chip fluorescent "standard", and was realized by illuminating through the microscope objective (20x) with UV light during 1 hour through the Pyrex wafer (see Figure 1B). In this work, we refer to "illumination" for long exposures (>1 min) of the sample to UV light, whereas we refer to "observation" for instantaneous (<1 s) exposure, necessary for image acquisition in the different channels. The goal of the standard is to provide an on-chip source of fluorescent signal, which would never be exposed again to additional illumination doses. Later we observe this fluorescence to correct for time-dependent variations in intensity of the fluorescent excitation source, as noted during long-term illuminations (see further). The location of the standard corresponds to the area Ω_{STD} in Figure 2. The standard and all reference patterns had a circular shape, achieved by programming the microscope to automatically close its diaphragm during illumination, and reopen it before observation.

In order to characterize in detail the fluorescence reference printing process, we performed several cycles of 60 s illumination steps nearby a previously printed standard and observed them in the UV/blue and the blue/green channels. A reference corresponds to the area Ω_R in Figure 2. The intensity of the light and the exposure time used for observation, were chosen such as to provide a significantly lower observation dose, compared to the illumination dose to avoid any alteration of the fluorescence of the standard and reference during observation. The printing experiments resulted in images as the one shown in Figure 2. The induced fluorescence, $I_{exc/em}$, read at any instant *t*, is calculated using the mean value of the pixel intensity from the different regions of interest from the obtained images, as described below.

First, we extract the mean pixel values of the *i* pixels p_i in each domain:

1. $p_i \in \Omega_R$, where Ω_R is the reference region, from which the extracted mean signal is $p_R(t)$.
2. $p_i \in \Omega_{STD}$, where Ω_{STD} is the standard region, from which the extracted mean signal is $p_{STD}(t)$.
3. $p_i \in \Omega_B$, where Ω_B is the background region without any Parylene-C, from which the extracted mean signal is $p_B(t)$.
4. $p_i \in \Omega_P$, where Ω_P is the non-illuminated region of Parylene-C, from which the extracted mean signal is $p_P(t)$.

The corrected induced fluorescence of the reference region is then calculated as follows:

$$I_{exc/em}(t) = \frac{p_R(t) - p_B(t)}{p_P(t) - p_B(t)} \qquad (1)$$

This method employed to calculate $I_{exc/em}$ allows us to compare the induced fluorescence in the region Ω_R with respect to the autofluorescence of the non-illuminated Parylene-C area (Ω_P). If only autofluorescence would be present (no printing is done), Eq. 1 is equal to one. To obtain the exact instantaneous illumination dose for a given time *t*, correcting for eventual fluctuations in time of the lamp intensity, we use following expression:

$$D(t) = D(t_0) \cdot \frac{p_{STD}(t)}{p_{STD}(t_0)} \qquad (2)$$

The second factor of Eq. 2 corrects for the time variations in the lamp intensity by comparing the signal in the standard area Ω_{STD} at every moment in time with the one at the beginning of the experiment. In this manner, by measuring the power of the lamp at the $t=t_0$, we could deduce the dose across the whole experiment. If the excitation intensity does not change over the time of duration of the experiment, the second factor simply becomes 1. The total dose is simply obtained by integrating the instantaneous doses over the duration of the experiment.

In order to see the effect of a long-term illumination and to extract data from different exposures, we programmed the microscope to illuminate the sample for fixed periods Δt of 60 s and to acquire the images in the different excitation/emission channels at every interval. We also set a mosaic acquisition experiment to perform the same illumination-observation sequence in six different positions of the chip, so as to reproduce the characterization several times. The same steps were repeated for 2, 5 and 10 μm thicknesses of the Parylene-C intermediate bonding layer. The resulting induced fluorescence values, as calculated using Eq. 1 and Eq. 2, are shown separately for the UV/blue (Figure 3A) and for the blue/green (Figure 3B) channels.

Concerning the UV/blue channel, the general observed trend consists of a fast increase of the induced fluorescence followed by a peak and a slower decay. In the case of 2 μm thickness, a maximum is reached at a total dose of 1050 J/cm^2, earlier than for the thicknesses of 5 and 10 μm, which show peak values at 1350 and 1450 J/cm^2, respectively. Considering that for a thicker layer, more fluorescent material is available, this result is expected. On the contrary, the value of the intensity of the peaks does not follow the same order: the maximum value of $I_{UV/blue}$ for 2, 5 and 10 μm are 2.51, 3.23 and 2.77, respectively. We believe that the reason for this relies on the depth of focus of the objective we used to illuminate the Parylene-C. The depth of focus (DOF) of the objective determines the volume where the light is focused and, thus, where the intensity is at the maximum. The DOF can be calculated as:

$$DOF = \frac{\lambda_0 n}{NA^2} + \frac{n}{M \cdot NA} e \qquad (3)$$

where λ_0 is the wavelength of the light (365 nm), n is the refractive index of air (1), NA is the numerical aperture of the objective (0.4) and e is the smallest feature that can be resolved by a detector that is placed in the image plane of the microscope objective (6.45 μm). The DOF of the 20x objective used for this experiment is then equal to 3.0 μm. When the Parylene-C layer is thinner than the DOF, the whole material is exposed to the maximum intensity. On the contrary, when the thickness of the Parylene-C is greater than the DOF, not all the Parylene-C is exposed in the same way, resulting in a partial exposure of the material.

Figure 3A indicates the fast initial generation of a fluorescent compound in the UV/blue excitation/emission channel as a function of the UV total writing dose, followed by a slower decay as typically observed during bleaching of a fluorophore. Figure 3B shows the fluorescence observed in the blue/green excitation/emission channel as a function of the total dose, also

revealing an increase in the signal followed by a decay, however with a less strong dependence on the dose than the curve of Figure 3A. This behaviour is further discussed in the Supplementary Information (SI) (see Figure S1).

Applications

The iPBLF can be used for several applications where the presence of a reference is required to interprete quantitatively fluorescent experiments and compare the results of different samples. For our microfluidic experiments, we printed a fluorescent reference dot nearby a microfluidic channel with the goal of having it on the same field of view as the fluorescent sample liquid flowing through the channel. In this manner, the fluorescence of the sample can be automatically compared to that of the fluorescent reference and, thus, to other experiments. In Figure 4, we define the areas of interest for calculating in a quantitative way the fluorescence signal of the liquid.. Similarly to the assessment of the dot printing above, we define the different regions of interest as follows:

1. $p_i \in \Omega_S$, where Ω_S is the sample region from which the extracted mean signal is p_S. This region is where the liquid sample to be analysed is located.
2. $p_i \in \Omega_R$, where Ω_R is the reference region, from which the extracted mean signal is p_R.
3. $p_i \in \Omega_P$, where Ω_P is the non-illuminated region of Parylene-C from which the extracted mean signal is p_P. This region is used to evaluate the autofluorescence of the background.

The induced fluorescence is then calculated as follows:

$$I_{exc/em} = \frac{p_S - p_P}{p_R - p_P} \quad (4)$$

With Eq. 4 we calculate the intensity of the sample under analysis with respect to the intensity of the reference dot. Note that, in this experiment, there is only 'observation' of the fluorescence and no UV 'illumination'. The latter was needed only for printing of the on-chip reference. Moreover, as we performed the fluorescent observation experiments in the stationary flow regime, we do not consider the time depence of Eq. 4.

Concentration sensor. In this experiment, we applied a stationary flow of different concentrations of FITC-labelled IgGs at 0.5 μL/s, corresponding to an average flow velocity of 170 mm/s, i.e. a fluorophore in the liquid stream on the average passes through the microchannel in 1.5 ms. Under these conditions, the fluorescent signal originating from the channel is uniform across its width and the flow rate was high enough to refresh the molecules in the channel so that the bleaching effect was insignificant, even though the lamp was continuously on.
Once the stationary flow conditions achieved (we start the experimental observation for safety at least 2 minutes after starting the flow), we acquired an image like the one shown in Figure 4 in the blue/green channel. We repeated the same experiments at different dilutions, the highest antibody concentration being 123 μg/mL. In order to compare the results obtained from the experiment under different external conditions, we ran the same set of experiments varying the excitation intensity (100, 50 and 25%) and the objectives used to acquire the images (20x and 10x). We then compared the intensity of the signal in the region Ω_S with and without making use of the reference dot. In the case in which no referencing was performed, the values of p_S were directly plotted against the normalized concentration (normalized by the highest value) of the antibodies (Figure 5A). However, when the signal obtained from the identical sample set was processed with Eq. 4, correcting the values with respect to the reference dot, a single linear plot (Figure 5B) was obtained, independent of the imaging parameters. This clearly demonstrates the efficiency of the on-chip programmed quantitative iPBLF reference in calibrating fluorescence intensity measurements.

Flow rate sensor. In this experiment, we lower the flow rate, at which we deliver the antibodies through the microfluidic channel until the bleaching rate and the molecules refreshment rate become comparable. Due to the parabolic profile, characteristic of liquid flowing in a channel driven by pressure, the rate of molecule refreshment in the centre of the channel is higher than the one closer to the edges. We consider a parabolic flow velocity in the channel as follows:

$$v(x) = k \cdot (w - x)x \quad (5)$$

with v the velocity in the channel, y the direction along the channel, x the direction across the channel and w its width. The middle of the channel, where $x = w/2$, corresponds to the maximum velocity of the flow and, thus, to the point where the refreshment rate is the highest. In order to visualize the parabolic flow profile, we plotted the fluorescent signal across the line A-A' of Figure 6A, which measures both the reference and the fluorescent signal of the liquid.. Figure 6B shows the parabolic-like profiles of the signal for a dilution of 1/100. We again use Eq. 4 to calculate $I_{blue/green}$, with p_S taken now as the value of the average pixel intensity for a given value of x along the line A-A'. The average values p_R and p_P are again used as the reference and background, respectively. The same profile was plotted for flow rates of 20, 15, 10, 8, 6, 4, 2 and 1 nL/s.
In order to find a relationship between the fluorescent intensity observed in the channel and the flow rate applied, we integrated $I_{blue/green}$ across the width of the channel: $A_{blue/green}(y) = \int_{-w/2}^{w/2} I_{blue/green}(x,y)dx$. The area $A_{blue/green}(y)$ under the curve obtained with this calculation represents the overall fluorescent intensity that results from the molecules that were still unbleached with blue light at a given y-position. In Figure 6C, we plotted the integrated signals $A_{blue/green}$ against the inverse of the flow rate Q^{-1}. The reason for this choice is that Q^{-1} gives a 'mean' time that the antibodies have spent under illumination, during which bleaching can occur. We also plotted the experimental results obtained when flowing the antibodies with a dilution of 1/200. We can clearly observe that there is a linear dependence of $A_{blue/green}$ with respect to Q^{-1}. Hence the measured value of $A_{blue/green}$ can be used to determine the flow rate, once calibration of the curve is done by applying a known flow rate for a given fluorescent molecule concentration.
Figure S2(A,B) of the SI presents a 3D plot showing the observed fluorescent intensity of the chip, including the reference dot and the microfluidic channel, for a flow rate of 20 nL/s and 4 nL/s, respectively. It shows that, while the intensity of the reference dot does essentially remains constant, the fluorescent intensity in the channel is observed to be clearly affected by the bleaching of the fluorophores.

Conclusions and Outlook

Quantitative programming of iPBLF proved to be very useful as an on-chip fluorescent reference, and opens ways to calibrate fluorescent intensity measurements using protocols of low complexity. The presented method eliminates the need for modifying fabrication flows and materials associated with the accommodation of the on-chip reference, and it can easily be scaled up to the wafer level by applying UV light with a mask aligner. Moreover, low-complexity processing algorithms allow multiple measurements, including but not limited to the demonstrated analyte concentration and the flow rate determination in a channel. We anticipate that point-of-care and mobile diagnostic applications that require the measurement of a fluorescent signal can benefit from the presented method in reducing the dependence of the outcome of the test on the skills of the operator and in simplifying the procedures required for calibration. Calibration of microfluidic chip protocols for enabling quantitative fluorescent measurements, in which inter- and intra-experiment variations are ruled out, is still lengthy and time-consuming, even in the laboratory. Quantitative programming of iPBLF can simplify and shorten these procedures, and is particularly of use for automatized biological experiments, where data collection with large image stacks is required.

Acknowledgements. The authors thank the National Competence Center for Biomedical Imaging (NCCBI) for the generous funding. We also thank the EPFL Center of Micronanotechnology for their valuable help during elaboration of the microfabrication procedure and members of the EPFL mechanical workshop for the technical assistance.

References

1. D. Mark, S. Haeberle, G. Roth, F. von Stetten, and R. Zengerle, *Chemical Society Reviews*, 2010, **39**, 1153.
2. T. Yang, S. Jung, H. Mao, and P. S. Cremer, *Analytical Chemistry*, 2001, **73**, 165–169.
3. I. Caelen, A. Bernard, D. Juncker, B. Michel, H. Heinzelmann, and E. Delamarche, *Langmuir*, 2000, **16**, 9125–9130.
4. S. Ghaemmaghami, W.-K. Huh, K. Bower, R. W. Howson, A. Belle, N. Dephoure, E. K. O'Shea, and J. S. Weissman, *Nature*, 2003, **425**, 737–741.
5. W. David E., in *Methods in Cell Biology*, pp. 63 – 91.
6. M. A. Model and K. E. Healy, *Journal of Biomedical Materials Research*, 2000, **50**, 90–96.
7. J. C. Waters, *The Journal of Cell Biology*, 2009, **185**, 1135–1148.
8. K. M. Kedziora, J. H. M. Prehn, J. Dobrucki, and T. Bernas, *Journal of Microscopy*, 2011, **244**, 101–111.
9. J. R. Swedlow, in *Methods in Cell Biology*, Elsevier, 2013, vol. 114, pp. 407–426.
10. L. Song, E. J. Hennink, I. T. Young, and H. J. Tanke, *Biophysical Journal*, 1995, **68**, 2588–2600.
11. M. Talhavini and T. D. Z. Atvars, *Journal of Photochemistry and Photobiology A: Chemistry*, 1998, **114**, 65–73.
12. J. M. Zwier, G. J. Van Rooij, J. W. Hofstraat, and G. J. Brakenhoff, *Journal of Microscopy*, 2004, **216**, 15–24.
13. J. M. Zwier, L. Oomen, L. Brocks, K. Jalink, and G. J. Brakenhoff, eds. J.-A. Conchello, C. J. Cogswell, and T. Wilson, 2007, p. 64430C–64430C–11.
14. J. M. Zwier, L. Oomen, L. Brocks, K. Jalink, and G. J. Brakenhoff, *Journal of Microscopy*, 2008, **231**, 59–69.
15. D. S. Baskin, M. A. Widmayer, and M. A. Sharpe, *Analytical Biochemistry*, 2010, **404**, 118–126.
16. S.-K. Hoi, X. Chen, V. S. Kumar, S. Homhuan, C.-H. Sow, and A. A. Bettiol, *Advanced Functional Materials*, 2011, **21**, 2847–2853.
17. A. T. Ciftlik and M. A. M. Gijs, *Journal of Micromechanics and Microengineering*, 2011, **21**, 035011.
18. A. T. Ciftlik and M. A. M. Gijs, *Lab on a Chip*, 2012, **12**, 396.
19. A. T. Ciftlik, D. G. Dupouy, and M. A. M. Gijs, *Lab on a Chip*, 2013, **13**, 1482.
20. D. G. Dupouy, A. T. Ciftlik, and M. Gijs, in *17th International Conference on Miniaturized Systems for Chemistry and Life Sciences (microTAS '13)*, 2013, pp. 260–262.

Notes

* Laboratory of Microsystems 2, École Polytechnique Fédérale de Lausanne, CH-1015 Lausanne, Switzerland. Fax: +41 21 693 59 50; Tel: +41 21 693 67 61; E-mail: martin.gijs@epfl.ch.

Figure Legends

Figure 1 Schematic view of the device lay-out. (**A**) Top view showing the microfluidic channel with in- and outlets. Several circular structures were etched together with the microfluidic channel in order to more uniformly distribute the pressure during bonding. (**B**) Schematic cross-section of the chip along the A-A' and B-B' profiles of Figure 1A, showing the position of the Parylene-C layer and the backside-etched hole for the inlet. For illumination and observation, the microscope objective is focused on the Parylene-C layer.

Figure 2 Fluorescent image observed in the blue/green channel showing a standard area (Ω_{STD}), an area without Parylene-C (Ω_B), an area with non-illuminated Parylene-C (Ω_P) and the illuminated reference area (Ω_R).

Figure 3 Characterization of the iPBLF in the reference area (Ω_R) under long-term illumination with UV for a 2, 5 and 10 μm thick layer of Parylene-C. The $I_{exc/em}(t)$ curves are obtained from the raw data by using Eq. 1 and Eq. 2 (**A**) Observation in the UV/blue channel, showing a fast increase in the signal, followed by a slower decay. (**B**) Observation in the blue/green channel, indicating an increase in the signal followed by a decay, however with a less strong dependence on the dose than the curve of Figure 3A.

Figure 4 Fluorescent image of the microfluidic channel and the on-chip reference, observed in the blue/green channel. The fluorescent signal of the solution flowing in the channel is obtained from the pixels in the area Ω_S and is referenced to the pixels of the area Ω_R by using Eq. 4.

Figure 5 Measurements of the fluorescent signal from a solution of FITC-labelled antibodies flowing in the microfluidic channel. The relative lamp power (P) and the objective magnification (M) are represented as follows: ■ P:100% M: 20x, ● P: 50% M: 20x, ▲ P:25% M:20x, ▼ P:100% M: 10x, ◆ P: 50% M: 10x ◀ P:25% M:10x. (**A**) Values of the average pixel intensity p_S from the area Ω_S plotted against the normalized concentration of the solution flowing in the microfluidic channel. (**B**) Values of $I_{blue/green}$ calculated using Eq. 4 and plotted versus the normalized concentration of the solution in the channel. The curve of this plot is independent on the different hardware configurations used for the experiment.

Figure 6 Measurements of the fluorescent signal from a solution of FITC-labelled antibodies flowing in the microfluidic channel under bleaching conditions (slow flow rate) with blue light. (**A**) Fluorescent

image of the microfluidic channel and the on-chip reference, observed in the blue/green channel. The fluorescent signal of the solution flowing in the channel is obtained from the pixels along the profile A-A' and is referenced to the area Ω_R by using Eq. 4. (**B**) Values of $I_{blue/green}$ across the profile A-A' for the flow rate Q taking the values of 20, 15, 10, 8, 6, 4, 2 and 1 nL/s, respectively. (**C**) The integrated intensity (area under the curve) across the channel, $A_{blue/green}$, as a function of Q^{-1} for two antibody concentrations (the 1/100 dilution corresponding to a concentration of 123 μg/mL).

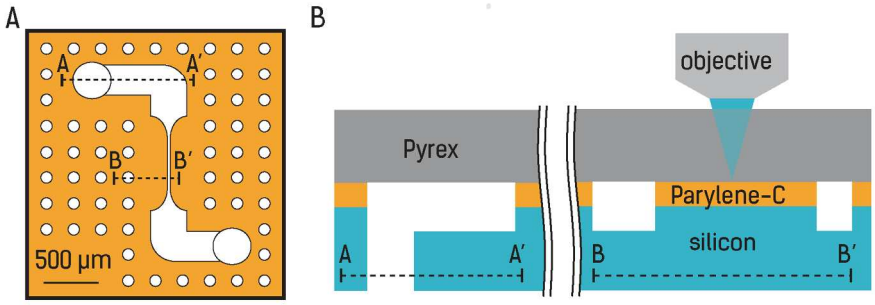

Figure 1 Schematic view of the device lay-out. (**A**) Top view showing the microfluidic channel with in- and outlets. Several circular structures were etched together with the microfluidic channel in order to more uniformly distribute the pressure during bonding. (**B**) Schematic cross-section of the chip along the A-A′ and B-B′ profiles of Figure 1A, showing the position of the Parylene-C layer and the backside-etched hole for the inlet. For illumination and observation, the microscope objective is focused on the Parylene-C layer.

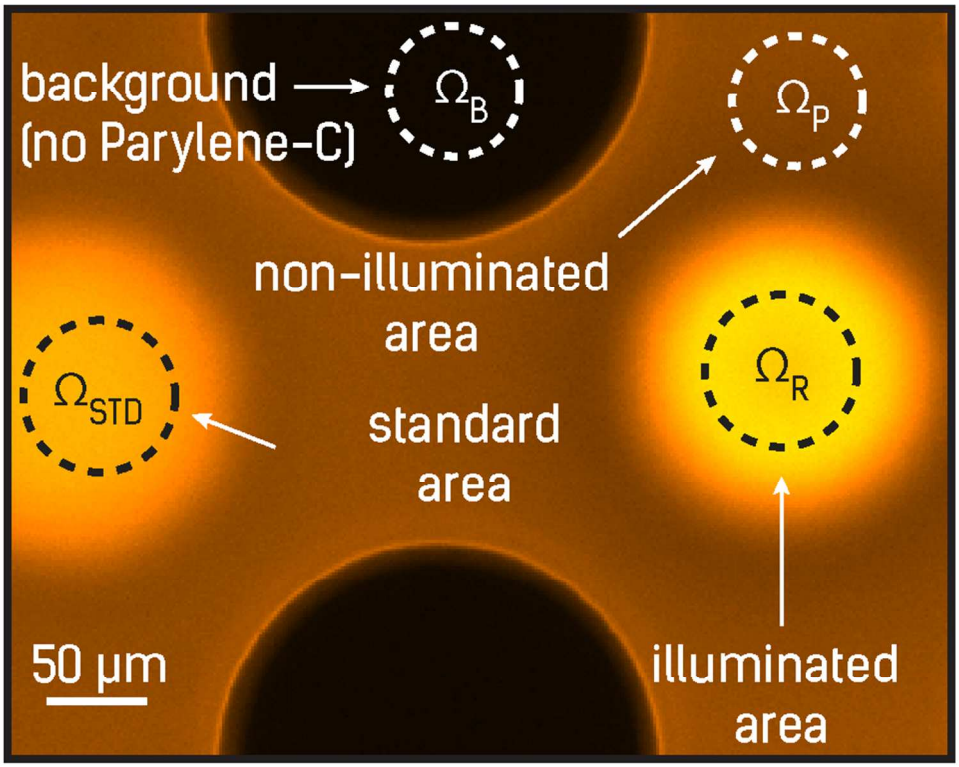

Figure 2 Fluorescent image observed in the blue/green channel showing a standard area (Ω_{STD}), an area without Parylene-C (Ω_B), an area with non-illuminated Parylene-C (Ω_P) and the illuminated reference area (Ω_R).

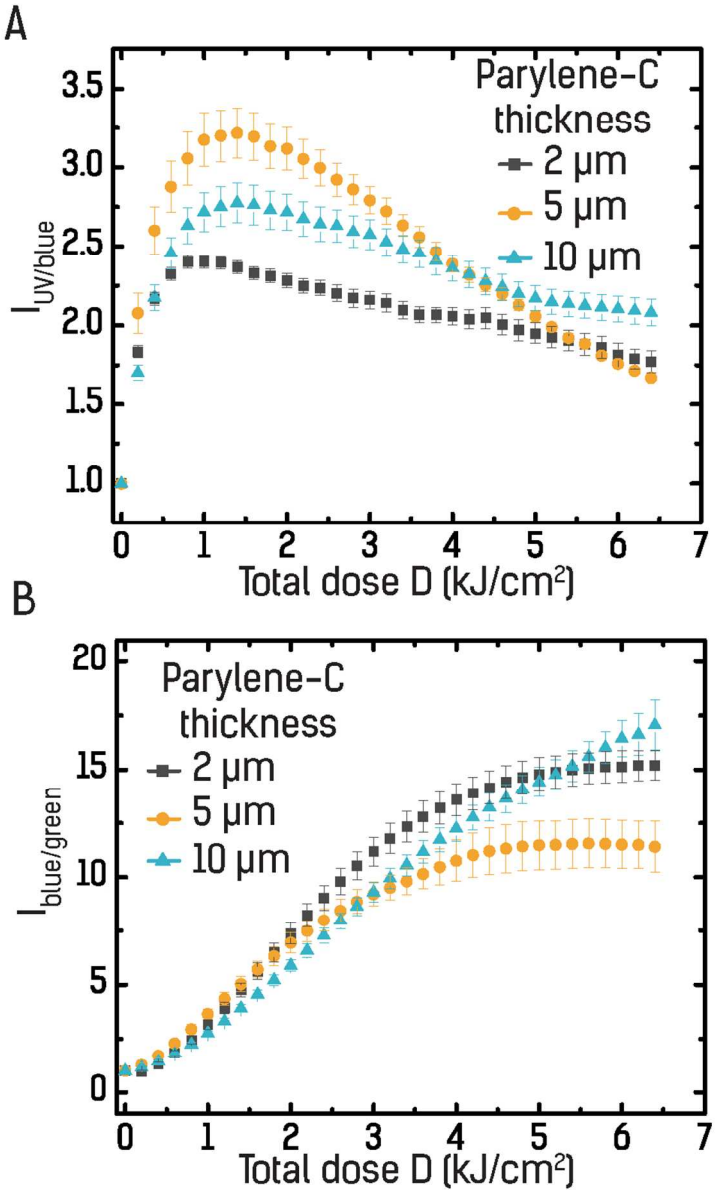

Figure 3 Characterization of the iPBLF in the reference area (Ω_R) under long-term illumination with UV for a 2, 5 and 10 µm thick layer of Parylene-C. The $I_{exc/em}$ (t) curves are obtained from the raw data by using Eq. 1 and Eq. 2 (**A**) Observation in the UV/blue channel, showing a fast increase in the signal, followed by a slower decay. (**B**) Observation in the blue/green channel, indicating an increase in the signal followed by a decay, however with a less strong dependence on the dose than the curve of Figure 3A.

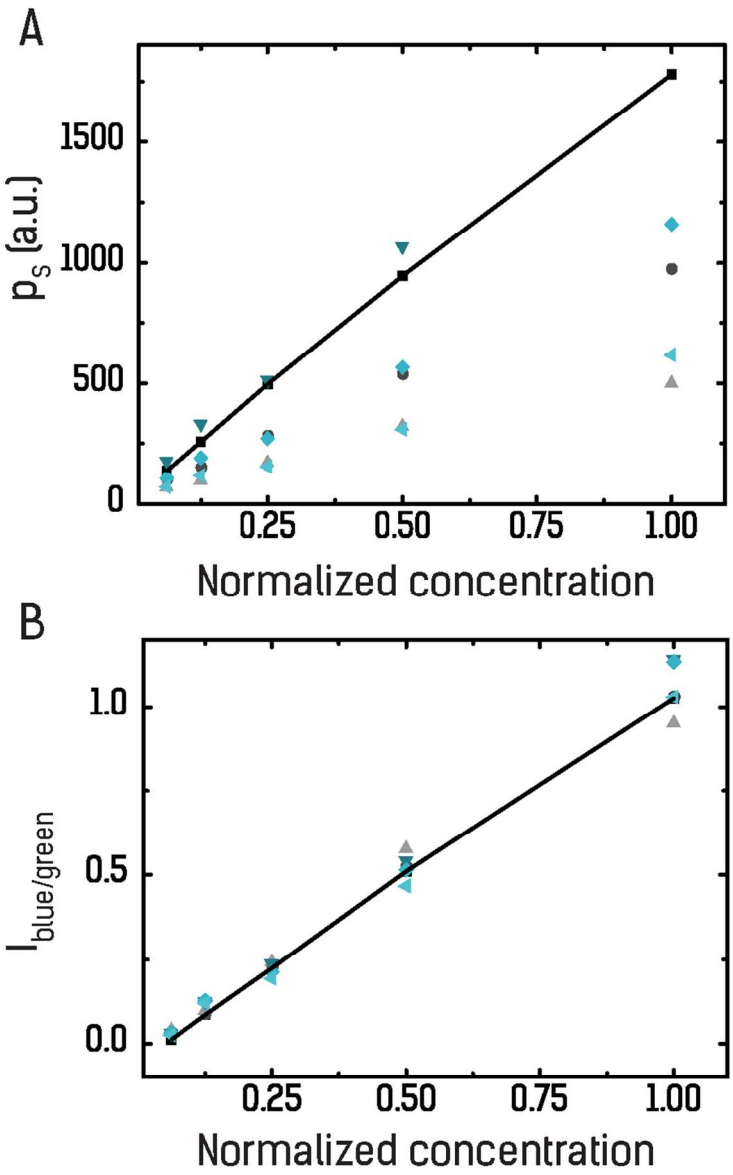

Figure 5 Measurements of the fluorescent signal from a solution of FITC-labelled antibodies flowing in the microfluidic channel. The relative lamp power (P) and the objective magnification (M) are represented as follows: P:100% M: 20x, P: 50% M: 20x, P:25% M:20x, P:100% M: 10x, P: 50% M: 10x P:25% M:10x. (**A**) Values of the average pixel intensity p_S from the area Ω_S plotted against the normalized concentration of the solution flowing in the microfluidic channel. (**B**) Values of $I_{blue/green}$ calculated using Eq. 4 and plotted versus the normalized concentration of the solution in the channel. The curve of this plot is independent on the different hardware configurations used for the experiment

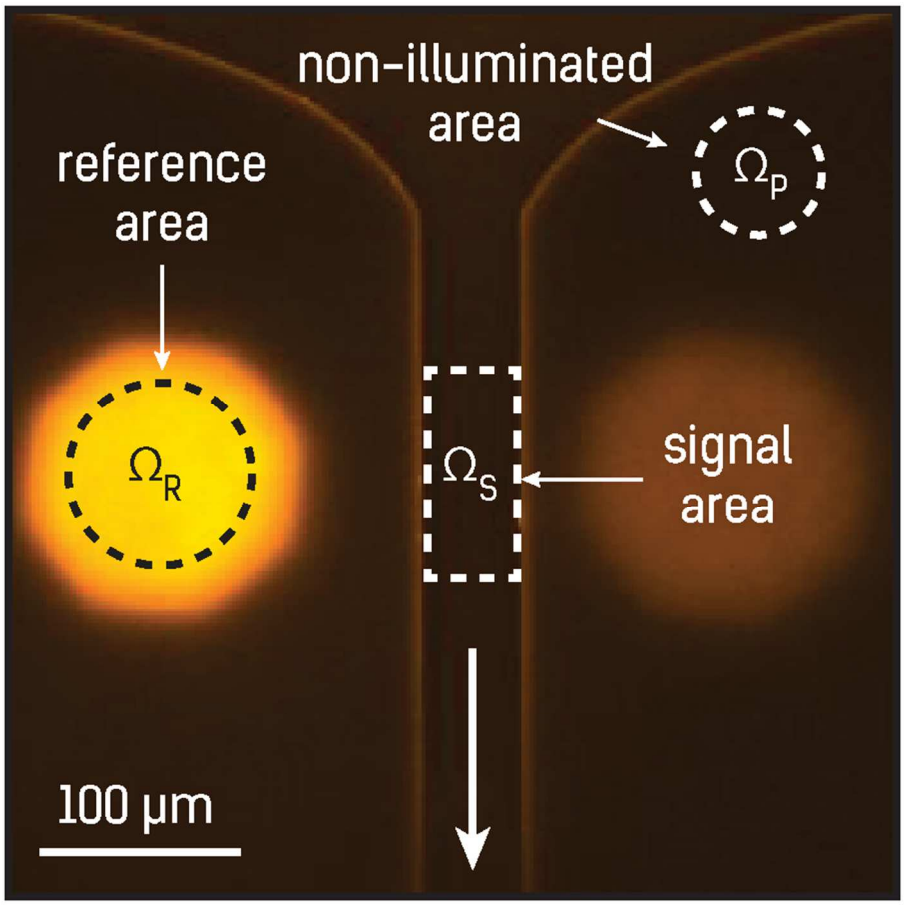

Figure 4 Fluorescent image of the microfluidic channel and the on-chip reference, observed in the blue/green channel. The fluorescent signal of the solution flowing in the channel is obtained from the pixels in the area Ω_S and is referenced to the pixels of the area Ω_R by using Eq. 4.

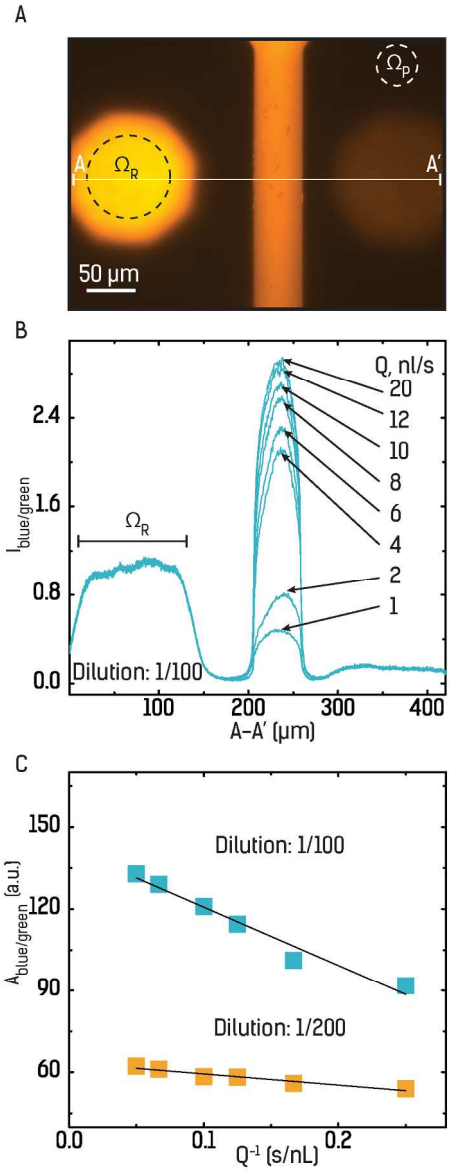

Figure 6 Measurements of the fluorescent signal from a solution of FITC-labelled antibodies flowing in the microfluidic channel under bleaching conditions (slow flow rate) with blue light. (**A**) Fluorescent image of the microfluidic channel and the on-chip reference, observed in the blue/green channel. The fluorescent signal of the solution flowing in the channel is obtained from the pixels along the profile A-A' and is referenced to the area Ω_R by using Eq. 4. (**B**) Values of $I_{blue/green}$ across the profile A-A' for the flow rate Q taking the values of 20, 15, 10, 8, 6, 4, 2 and 1 nL/s, respectively. (**C**) The integrated intensity (area under the curve) across the channel, $A_{blue/green}$, as a function of Q^{-1} for two antibody concentrations (the 1/100 dilution corresponding to a concentration of 123 µg/mL).